Charge transfer and structure in C_{60} adsorption on metal surfaces

M. R. C. Hunt
Cavendish Laboratory, Madingley Road, Cambridge CB3 0HE, United Kingdom
and Laboratorio Tecnologie Avanzate Superfici e Catalisi, Istituto Nazionale per la Fisica della Materia, Padriciano 99, I-34012 Trieste, Italy

S. Modesti
Laboratorio Tecnologie Avanzate Superfici e Catalisi, Istituto Nazionale per la Fisica della Materia, Padriciano 99, I-34012 Trieste, Italy
and Dipartimento di Fisica, Università di Trieste, I-34127 Trieste, Italy

P. Rudolf
Laboratorio Tecnologie Avanzate Superfici e Catalisi, Istituto Nazionale per la Fisica della Materia, Padriciano 99, I-34012 Trieste, Italy

R. E. Palmer
Cavendish Laboratory, Madingley Road, Cambridge CB3 0HE, United Kingdom
(Received 24 October 1994)

The charge state and structure of C_{60} monolayers deposited on Au(110), polycrystalline Ag, and Ni(110) have been investigated by electron-energy-loss spectroscopy and low-energy electron diffraction. The vibrational excitation spectra have been used to obtain a quantitative determination of the molecular charge state of the adsorbed C_{60} molecules. On both the Au(110) and Ag surfaces the charge transfer from the surface to the C_{60} is found to be (1 ± 1) electrons and that on Ni(110) is (2 ± 1) electrons. These estimates are supported by the metallic nature of the low-energy (0–7.5 eV) electronic excitations of the monolayers. For submonolayer coverages of C_{60}, rectangular overlayer phases are observed on Ni(110) in contrast to the close-packed islands seen on the other metals. This difference in the low-coverage structure can be related to differing substrate-adsorbate interactions, directly reflected by the C_{60} charge state.

INTRODUCTION

The early stages of growth of C_{60} on a surface, and especially the nature of the interaction of the first fullerene monolayer with that substrate, are of great interest from both a fundamental and an applied viewpoint. The optical[1–3] and electronic[4–6] properties of the fullerenes, including superconductivity,[7–11] depend intimately on the charge state of the fullerene molecule and are likely to be significantly influenced by the crystalline structure. It has been discovered, for example, that there are two distinct families[10] of fullerene-based superconductors, with different crystalline symmetries and which have different dependences of the critical temperature upon lattice parameter. By discovery of the means to control both charge state and the crystalline structure, we can determine the essential elements required for the creation of the superconducting state.

In this paper we present the results of a detailed study of the electronic and structural properties of submonolayer and monolayer coverages of C_{60} on three metal surfaces. Two noble metals, Au(111) and polycrystalline Ag, and a transition metal, Ni(110), were chosen in order to compare the charge transfer to, and structure of, C_{60} adsorbed on surfaces with differing work functions [Au(110), 5.37 eV; polycrystalline Ag, $\approx$4.6 eV; Ni(110) 5.04 eV (Ref. 12)] and reactivity. The charge state of the adsorbed C_{60} molecules was obtained quantitatively by analysis of the softening of the molecular vibrational modes upon adsorption. Support for the charge states determined in this manner was provided by low-energy electronic excitation spectra (0–7.5 eV) of the overlayers, which were clearly metallic.

EXPERIMENT

The experiments were carried out in an ultrahigh-vacuum (UHV) system consisting of a preparation and an instrumentation chamber which had base pressures of 1×10^{-10} and 5×10^{-11} mbar, respectively. The samples were prepared by cycles of Ne^+ ion sputtering and annealing. Additional cycles of baking to 870 K first in 1×10^{-8} mbar of oxygen for 25 min and then in 1×10^{-8} mbar hydrogen for 15 min were required after the sputtering cycles to completely clean the Ni(110) sample. Sample cleanliness was monitored by a Varian cylindrical mirror analyzer (CMA) Auger electron spectrometer (AES), which was also used to determine adsorbate coverage from the ratio of substrate and overlayer Auger peaks. The coverage was calibrated by measuring the Auger peak ratios at monolayer coverage, produced by saturating the surface at a temperature ($\approx$600 K) above

that required for desorption of the multilayer. For Au(110) the ratios of the carbon *KLL* peak at 272 eV to the Au peaks at 69 and 356 eV were used, on Ag the ratio of the 272 eV peak to the 351 and 356 eV peaks, and for Ni the ratio of the carbon peak to the 61, 102, 848, and 865 eV peaks. Ratios of overlayer to substrate Auger peaks were taken for substrate peaks at a number of energies to minimize intensity variations which could arise due to slight differences in sample orientation during the acquisition of different Auger spectra. An Omicron low-energy electron-diffraction (LEED) optics, which like the CMA was mounted in the preparation chamber, was used to determine surface symmetry.

99% pure C_{60}, obtained from Texas Fullerenes, was sublimated from a tantalum crucible at around 700 K onto the samples, the temperature of which could be carefully controlled by resistive heating. A shutter between the source and sample was used to control the deposition time. The pressure during dosing remained between 5×10^{-10} and 1×10^{-9} mbar. After preparation of the sample and characterization by LEED and AES, the vibrational and electronic excitations of the surface could be measured using a Leybold-Hereaus ELS-22 high-resolution electron-energy-loss spectrometer (HREELS) mounted in the instrumentation chamber. The HREELS also provided a second means of measuring sample cleanliness more sensitive than that provided by the CMA. Vibrational spectra were acquired at a beam energy of 2 eV (10 eV) with an incident angle of 72° with respect to the surface normal and an analyzer angle of 72° ($\approx$20°) for on- (off-) specular scans. Electronic excitation spectra were acquired in the specular geometry, with incidence and reflection angles of 72° at an incident beam energy of 10 eV. All spectra were obtained at room temperature.

RESULTS AND DISCUSSION

The growth of C_{60} on the Au(110) and the Ag(110) surfaces has already been the subject of detailed studies with the scanning tunneling microscope (STM).[13,14] Upon adsorption of C_{60} and annealing to temperatures of 700 K the Au(110) surface undergoes an adsorbate-induced modification of the existing reconstruction[13,14] which leads to a close-packed C_{60} monolayer which has (6×5) periodicity with respect to the unreconstructed substrate. No such reconstruction is observed for adsorption onto the unreconstructed Ag(110) surface. For submonolayer C_{60} coverages on both surfaces the adsorbate is seen to form close-packed, two-dimensional islands, which nucleate preferentially at terrace sites. These islands then grow steadily with coverage to form a complete close-packed monolayer of C_{60} molecules. No other structural phases are observed on these surfaces. The nucleation of close-packed islands at terraces on these surfaces is in contrast to the nucleation at step edges observed on Cu(111), Ag(111), and in the early stages of growth on Au(111),[14–17] and can be explained in terms of a preference of the fullerene molecules for more open, and hence reactive, regions of the metal surface.

The polycrystalline Ag sample used showed a clear region of well-defined crystallinity corresponding to the (111) plane of the surface, 7×5 mm^2 in area (total sample area was approximately 300 mm^2). Monolayers of C_{60} grown on this sample showed a sharp, single-domain, hexagonal diffraction pattern in the ordered region. Coupled with the observation of a strong specular HREELS beam and the changes in the relative intensities of dipole-active and -forbidden molecular vibrational modes, which will be discussed in more detail below, this leads to the conclusion that the C_{60} formed a well-ordered monolayer on the Ag surface. For monolayer coverages of C_{60} on Au(110), the (6×5) periodicity observed[13,14] with the STM was clearly seen with LEED for deposition and annealing temperatures above 500 K. For adsorption at lower temperatures a hexagonal LEED pattern corresponding to a close-packed C_{60} layer without modification of the substrate surface reconstruction was observed. A weak hexagonal diffraction pattern was observed even for deposition with the substrate at room temperature, indicating the relatively high mobility of the C_{60} molecules on the Au(110) surface.

C_{60} growth on the Ni(110) surface produces three phases, one commensurate with the substrate, one partly commensurate, and one exhibiting a domain structure, indicating that there is a stronger substrate-adsorbate interaction than that observed for the noble-metal surfaces. For Ni substrate temperatures below 540 K, no order can be observed by LEED for any coverage below the multilayer, which contrasts to growth on Au(110), where clear evidence of an ordered overlayer can be seen at room temperature. Even dosing between 540 and 600 K produces only a poor-quality LEED pattern, consisting of a hexagonally ordered array of broad spots, indicative of order on a rather localized scale. It is only for growth at higher substrate temperatures that clear diffraction patterns can be obtained.

When growth occurs at sample temperatures above 620 K a strong diffraction pattern characteristic of a (5×3) overlayer [Fig. 1(a)] can clearly be observed from coverages above 0.15 ML. All coverages quoted in this paper are with respect to a saturated hexagonal C_{60} monolayer, i.e., a *physical* monolayer rather than a ratio of adsorbed molecules to substrate surface atoms. The appearance of this diffraction pattern at coverages much lower than the (5×3) saturation coverage of 0.74 ML indicates that growth occurs through island formation. The (5×3) islands have a rectangular lattice and a molecule-molecule spacing of 10.5 Å in the substrate [001] direction and 12.4 Å parallel to the $[1\bar{1}0]$ direction [Fig. 2(a)]. These nearest-neighbor distances are much larger than the spacing of 10.03 Å observed[18] in bulk, undoped C_{60}. The large difference in spacing relative to the bulk material is further evidence of a strong substrate-adsorbate bond compared with those to the noble-metal,[13–17,19] graphite,[20] and some semiconductor[21] surfaces on which only closed-packed, hexagonal, or quasihexagonal C_{60} structures are observed, even at the lowest coverages.

If the coverage of C_{60} is increased above 0.5 ML the nucleation of one of two phases, both of which possess a quasihexagonal symmetry, is observed. The phase which is adopted by the overlayer is strongly dependent on the

substrate temperature during the growth process. For low growth temperatures (between 630 and 660 K) a diffraction pattern characteristic of a single-domain quasihexaganal phase (Fig. 3) is observed (the QH1 phase). In this phase the $[1\bar{1}0]$ direction of the C_{60} lattice [assuming an equivalence between the quasihexagonal overlayer and the fcc (111) close-packed plane of C_{60}] is parallel to the $[1\bar{1}0]$ direction of the Ni(110) surface [Fig. 2(c)]. This direction is parallel to the troughs of the (110) fcc surface. LEED patterns show that this phase is commensurate with the substrate in the [001] direction, which from purely geometrical arguments would be the direction in which the substrate corrugation is likely to be the greatest. A similar uniaxially commensurate C_{60} overlayer is observed on the Au(001) surface.[19] The commensurate nature of the C_{60} layer in the [001] direction of the Ni(110) surface suggests that there is a preferential diffusion of the C_{60} molecules along the $[1\bar{1}0]$ troughs [Fig. 2(b)]. Such an overlayer geometry would lead to a dilation of the intermolecular spacing in the $[0\bar{1}1]$ direction of the C_{60} overlayer of the order of 16% compared to the bulk spacing.[18] This is a very considerable lattice strain, and is a striking illustration of the strength of the C_{60}-nickel bond. Further evidence for the strength of the chemisorption bond comes from the nucleation of close-packed structures at coverages of only about two-thirds of a saturated (5×3) overlayer, which indicates that there are significant fluctuations of adsorbate density over the surface. Such density fluctuations can only be attributed to the relative lack of mobility of C_{60} on Ni(110) in comparison to the other metal surfaces.

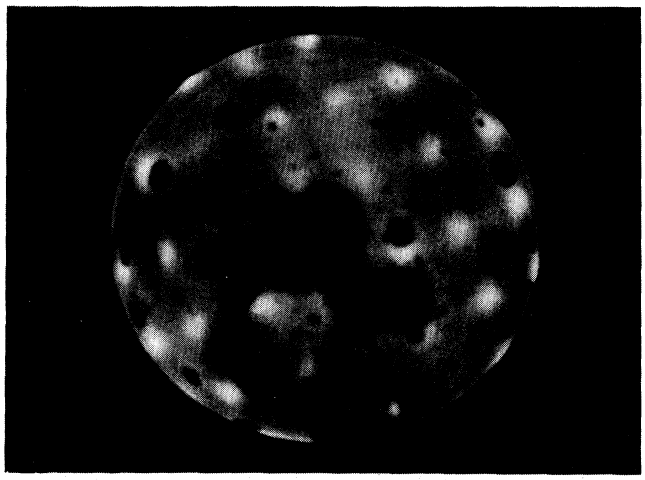

(a)

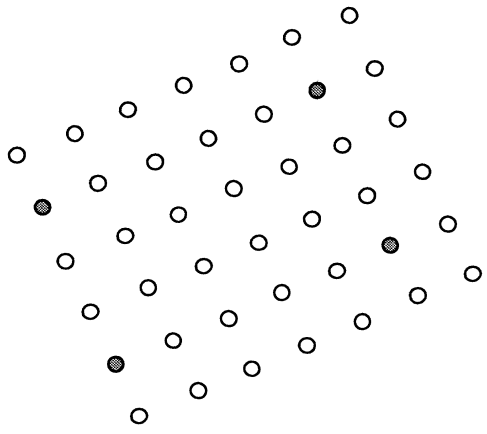

(b)

FIG. 1. (a) LEED pattern and (b) schematic of (5×3) C_{60}/Ni(110). Shaded circles represent the positions of diffraction spots from the clean Ni(110) surface. The incident beam energy was 26 eV.

When C_{60} is deposited at coverages beyond 0.5 ML at substrate temperatures between 660 and 720 K a diffraction pattern showing two distinct quasihexagonal domains (QH2) rotated at 30° to one another (Fig. 4), is observed. Dosing or annealing at higher temperatures leads to the decomposition of the C_{60} molecules.[22] Although the QH2 domains are produced by substrate growth at high temperatures, reducing the substrate temperature slowly (over a period of an hour) to the lower growth temperature or annealing the single-domain phase to the higher temperature does not produce any phase transformation. The formation of similar rotated domains at elevated temperatures is observed in RHEED studies of the growth of C_{60} on CaF_2.[23] However, in the case of this system the formation of the rotated domains at higher temperatures leads to a significant reduction in the lattice mismatch between substrate and overlayer, and neither of the rotated domains corresponded to the original uniaxial domain. The driving force for domain formation on the Ni(110) at monolayer coverages can, in contrast, only be attributed to the ability of the C_{60} molecules to surmount the higher diffusion barrier presented by the surface in the [001] direction than in the $[1\bar{1}0]$ direction at the higher growth temperature. A schematic illustration of this mechanism is given in Fig. 2 by the progression from Fig. 2(a) through 2(d), leading to the formation of the structure shown in Fig. 2(e).

In order to quantify the interaction of C_{60} with metal substrates in terms of charge transfer we have measured the substrate-induced shifts of some of the vibrational modes of the molecule. The softening of a vibrational mode of C_{60} with charge transfer is dependent on the mode symmetry and eigenvector,[24] as explained below, and is therefore not the same for each. To differentiate between the modes we use the fact that when obtained in a specular geometry HREEL spectra are dominated by excitations which satisfy the dipole selection rule,[25] and in consequence the ir-active vibrational modes present

the strongest spectral features in the vibrational region (Fig. 5). This is clearly seen by the decrease in relative intensity of dipole-allowed vibrational excitations in spectra obtained in the off-specular geometry (Fig. 6). In the bottom curve of Fig. 5 we show a HREEL spectrum obtained from an ordered 5 ML C_{60} film deposited on Au(110); the form of the spectrum is the same as that observed from ordered multilayers on other substrates.[26] The main peaks at 66, 146, and 178 meV and the shoulder at 71 meV correspond to dipole-active T_{1u} modes.[27,28] The spectrum in Fig. 6(a) is obtained from the same film with HREELS analyzer 50° off specular. In principle all the vibrational modes of the molecule can be excited in this geometry, so assignments can only be made by direct comparison with the vibrational frequencies obtained from bulk C_{60} by other experimental methods. Using results from Raman scattering,[27,29–31] we can assign the highest-lying observed mode as the Raman-active $H_g(8)$ mode (to adopt the notation used in Refs. 30–32) with a possible contribution from the $H_u(7)$ and $T_{2u}(5)$ modes, which a recent first-principles study of the vibrational modes of an isolated C_{60} molecule[32] found to be of similar frequency. We obtain the peak positions for both on- and off-specular spectra using a nonlinear least-squares fit with Gaussian line shapes, which produced an error in peak positions of ± 0.5 meV. Fits with other line shapes (i.e., Gaussian-Lorentzian products) produced the same results to within the fit error. A recent theoretical calculation[33] based on a unified interaction model, has shown that in bulk C_{60} dispersion greater than the error on the least-squares fits used to produce the results presented here only occurs for one mode lying above about 40 meV. These dispersions are in agreement with our analysis of the on- and off-specular spectra obtained from the 5 ML C_{60} film, which show no dispersion for detectable modes above 40 meV (the mode predicted to disperse is not visible in our spectra).

When a monolayer of C_{60} is adsorbed on the Au(110) or polycrystalline Ag surfaces a shift of -3 meV is observed in the lowest-lying T_{1u} mode, with no shift ob-

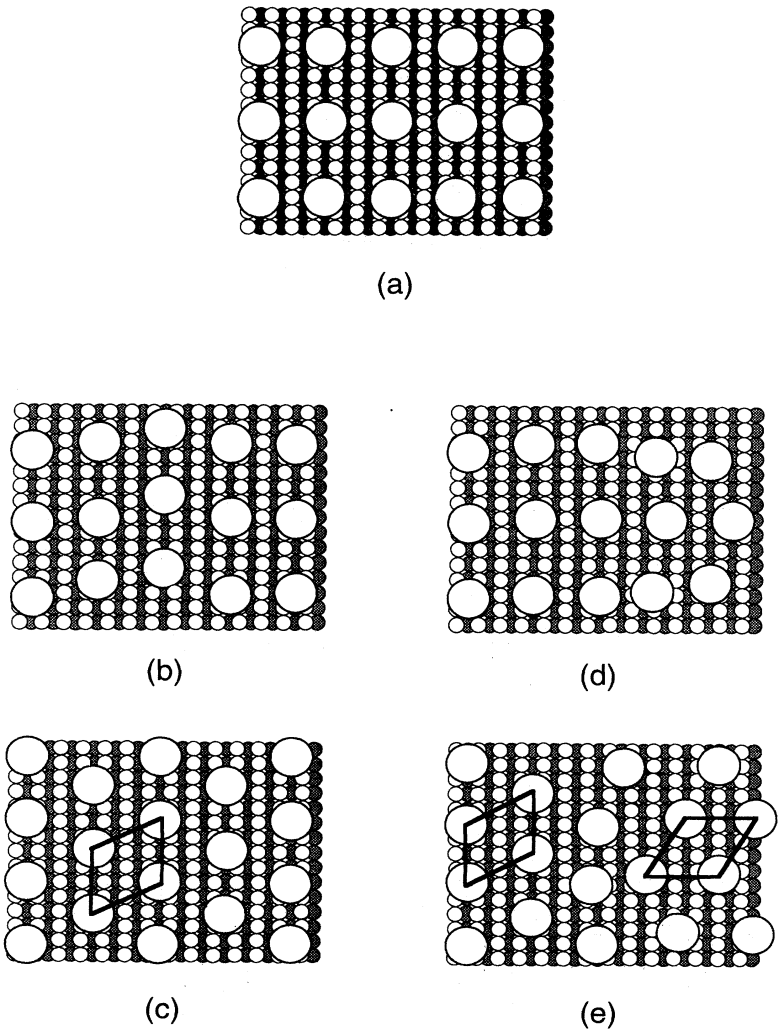

FIG. 2. Schematic representation of the phases of a C_{60} overlayer on Ni(110). (b) and (d) are intermediates between phase (a) and phases (c) and (e), respectively. See the text for details.

served in the higher-lying dipole-active modes (Fig. 5). The highest-lying dipole-forbidden mode, at 193 meV in the C_{60} multilayer, is observed to shift downward by 0.5 meV upon adsorption on Au(110) (Fig. 6), which agrees closely with the shift observed in the $H_g(8)$ mode by a Raman study of monolayer C_{60} on a polycrystalline Au film[30] (-0.74 meV). One clearly observes a greater shift in the positions of the vibrational modes of C_{60} for adsorption on Ni(110) than for the noble metals. HREEL spectra from the (5×3) and QH phases on Ni(110) are similar and indicate the same C_{60} charge state. Therefore the C_{60} charge state is seen not to be sensitive to coordination of the adsorbed C_{60} with the substrate. The observed frequency shifts for C_{60}/Ni(110) are -4 meV for the first dipole-active mode, -3 meV for the highest-frequency dipole-active mode, and -4.5 meV for the highest-lying mode.

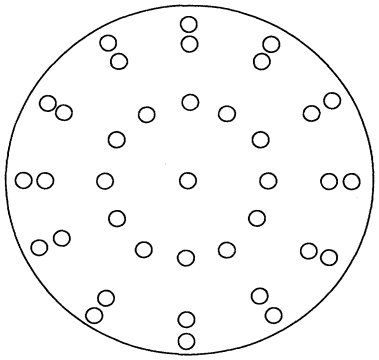

FIG. 4. Schematic LEED pattern from the QH2 phase of C_{60}/Ni(110). The solid circle marks the extent of the LEED screen. Incident beam energy was 23 eV.

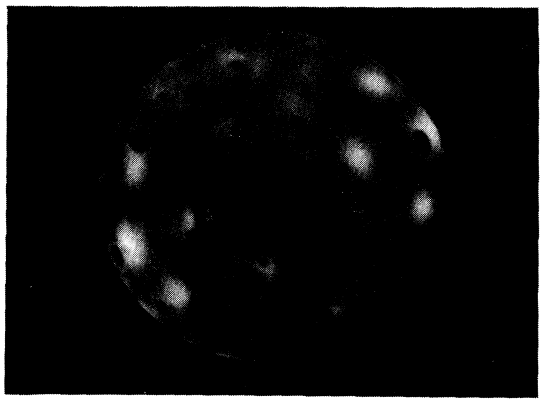

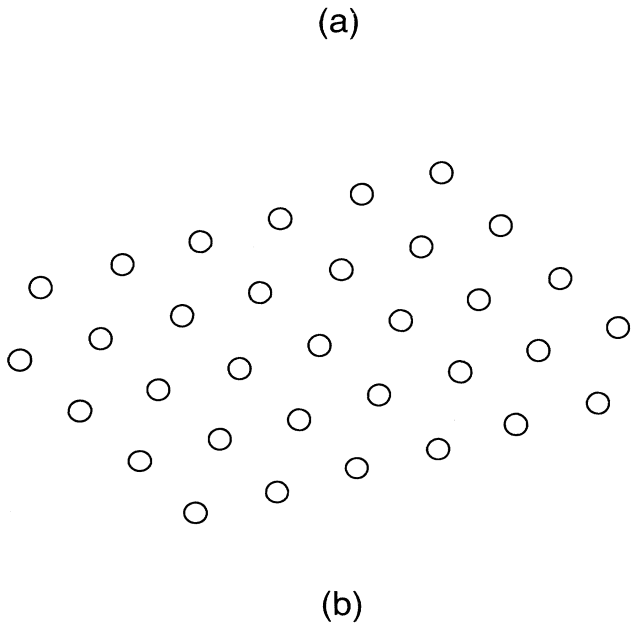

FIG. 3. (a) LEED pattern and (b) schematic of the QH1 phase of C_{60}/Ni(110). Incident beam energy was 24 eV.

Rice and Choi[34] have, in a recent theoretical study, proposed that the frequency of the ir-active vibrational modes of the C_{60} molecule should shift significantly with charge transfer due to coupling of the vibrations with virtual t_{1u}-t_{1g} electronic transitions. Moreover, the observed frequency shift should be in direct proportion to the number of electrons transferred to the molecule (-1.8 meV per electron for the mode at 178 meV), and an enhancement of the integrated signal strength quadratically dependent upon this charge transfer should occur. *Ab initio* molecular-dynamics calculations[35] predict that there should be different shifts in frequency with transferred charge for each of the T_{1u} modes, and that only the highest- and lowest-energy dipole-active modes

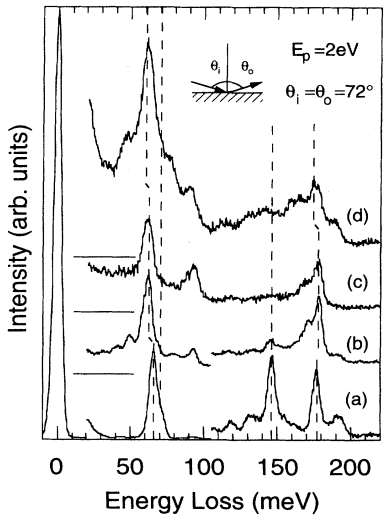

FIG. 5. HREEL spectra obtained in the specular geometry of (a) a multilayer C_{60} film (×12 and ×250), and monolayers of C_{60} on (b) Au(110) (×125 and ×250), (c) polycrystalline Ag (×125), and (d) Ni(110) (×150). Solid lines indicate the zero level of the spectra. The spectra are normalized to the specular elastic peak.

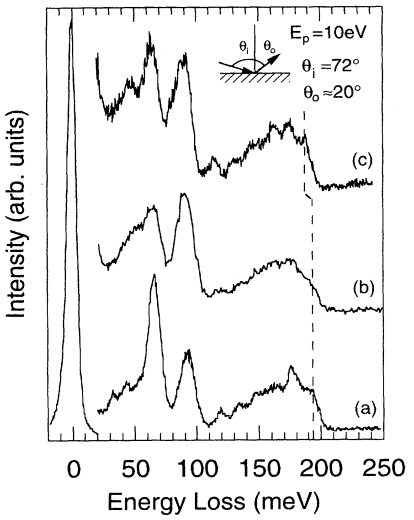

FIG. 6. HREEL spectra, obtained in an off-specular (72°,20°) geometry, of (a) a multilayer C_{60} film, (b) a monolayer of C_{60} on Au(110), and (c) a monolayer of C_{60} on Ni(110). (All spectra are ×7.)

should soften, in agreement with results of infrared absorption spectroscopy (IRAS) experiments on bulk C_{60} compounds,[28,36] a previous HREELS study[37] of alkali metal and C_{60} coadsorption, and the results presented here. In the IRAS study, Pichler and co-workers[28,36] measured the variation of the infrared-active vibrations of bulk C_{60} as a function of doping with alkali metal, and found an excellent agreement between the experimental data and theoretical prediction, particularly in regard to frequency shift. An almost linear shift in charge transfer of -1.25 meV per electron for the first mode and -1.8 meV per electron for the fourth mode is observed. This change in vibrational frequencies is large enough to be easily detected by HREELS.

The molecular-dynamics calculations[35] also show a significant shift in the frequency of some of the dipole-forbidden vibrational modes, which is supported by the results of Raman scattering[29,30] from bulk, doped films, and from submonolayers and monolayers of C_{60} adsorbed at noble-metal surfaces.[31] The shift in frequency with charge state observed for dipole-allowed and dipole-forbidden modes can be viewed in terms of changes in the intramolecular carbon-carbon bond length in the C_{60} molecule.[30,35] Upon charge transfer both theoretical[35,38] and experimental results[10] show a significant change in the bond lengths within the fullerene molecule. The transferred charge can be regarded as possessing an antibonding character with respect to the carbon-carbon double bonds and a bonding character with respect to the single bonds. Extra charge density leads to an expansion of the double bonds from 1.39 to 1.43 Å and a contraction of single bonds from 1.45 to 1.43 Å in Na_2CsC_{60}.[10] The modes most sensitive to the change in bond lengths are the tangential modes which involve stretching the double bonds of the molecule[29,30] and in consequence the higher-lying Raman-active modes are particularly affected: the highest-lying $H_g(8)$ mode manifests a frequency shift of -1.85 meV per electron, assuming a linear variation of frequency with charge state, whereas the radial $H_g(4)$ mode at 94.8 meV shifts at a rate of -0.25 meV per electron. The highest- and lowest-frequency dipole-active T_{1u} modes also involve bending and stretching primarily the double bonds of the molecule and therefore upon charge transfer they shift downward in frequency, while the other two T_{1u} modes involve deformation of both double and single bonds and hence do not shift significantly.

Applying these results, we can obtain a quantitative estimate of the C_{60} charge state from the vibrational frequency shifts which are observed upon adsorption at the Au(110), polycrystalline Ag, and Ni(110) surfaces. The charge transfer to C_{60} molecules on the noble-metal surfaces is 0 ± 0.7 electrons, based on the absence of a shift in the highest-lying dipole-active mode and 2.3 ± 0.7 electrons based on the shift of -3 meV of the lowest-frequency T_{1u} mode. The discrepancies between the charge states which are obtained from examination of different modes are due to some nonlinearity in the frequency shifts, most probably caused by an anisotropic distortion of the molecule brought about by bonding with the surface.[39] The downshift of the highest-lying dipole-forbidden mode, from 193 meV in the C_{60} multilayer, to 192.5 meV upon adsorption on Au(110), indicates a charge transfer of 0.5 ± 0.7 electrons per molecule, if we assume that all modes contributing to this peak downshift at an equal rate [equal to that of the $H_g(8)$ mode]. The C_{60} charge state obtained in this manner can be compared to the values of 0.4 and 0.9 electrons per molecule for adsorption of C_{60} monolayers on polycrystalline Au and Ag, respectively, obtained from the data of Chase *et al.*[31] Evidence that the downshift of the vibrational modes of the C_{60} molecules is the result of charge transfer *to* the molecules is provided by the bias dependence of the shifts of the highest-lying molecular modes for C_{60} layers on noble-metal electrodes.[40,41] Application of a negative bias to an electrode coated with a 1 or 2 ML C_{60} film leads to a greater reduction in the frequency of higher-lying Raman-active modes, consistent with a greater degree of charge transfer from surface to adsorbate. We can therefore safely conclude that the charge transfer to C_{60} molecules deposited on the noble-metal surfaces is between 0 and 2 electrons, with a value of 0.9 electrons provided by the average of our results.

The structural data detailed above indicate that there is a stronger interaction between the adsorbed C_{60} and the Ni(110) surface than with the noble-metal surfaces. C 1*s* core-level spectra reported by Ohno *et al.*[42] also provide evidence for a stronger interaction of the C_{60} with transition-metal surfaces (polycrystalline Cr) than with those of noble metals (polycrystalline Au). This assertion is borne out by a determination of charge transfer from the HREEL spectra that we have obtained. The frequency shift for C_{60}/Ni(110) of -3.5 meV for the first dipole-active mode indicates a transfer of 2.8 ± 0.7 electrons per molecule from the surface. The shift -3 meV for the highest-frequency dipole-active mode gives a charge

transfer of 1.7 ± 0.7 electrons, and that of -4.5 meV for the highest-frequency mode shows a transfer of 2.5 ± 0.7 electrons per molecule. From these results we can infer that between 1 and 3 electrons are transferred from the Ni(110) surface to each C_{60} molecule, with an average value of 2.3 electrons per molecule.

Frequency shifts similar to those discussed in this paper have been observed for monolayer C_{60} adsorbed on Rh(111),[43] indicating a strong chemisorption bond between the C_{60} and the Rh(111) surface. These results may also be interpreted in terms of the charge-transfer formalism developed in this paper,[44] involving a net transfer of charge to the adsorbate.

The electronic excitation spectrum of C_{60} monolayers also shows a dramatic dependence on the C_{60} charge state. In the geometry and at the primary beam energies used to obtain the spectra they are almost completely dominated by the response function of the C_{60} layer, as is indicated by the absence of the strong Ag surface plasmon peak for monolayer C_{60}/Ag, shown in Fig. 7(c), and the similarity in the energies of the broad maxima in the spectra of monolayer C_{60} on Au(110), Ni(110), and Ag (about 0.8, 3.2, 4.5, and 6.5 eV). A multilayer (5 ML) film of C_{60} is clearly semiconducting, and exhibits a band gap of about 2 eV [Fig. 7(a)]. A series of sharp, dipole-forbidden, excitonic peaks can be observed in the 1.5–2 eV region (marked with arrows) and band-to-band transitions are seen which are at energies in close agreement with those in the literature,[45,46] and with the loss function computed from the C_{60} dielectric functions.[47] The excitation spectra for a monolayer of C_{60} on all the metal surfaces are metallic, without the presence of excitonic features or a band gap [Figs. 7(b)–7(d)], in agreement with photoemission data[22,31,39,41] and EEL spectra[37,48] of monolayers on a wide variety of metal substrates. Any gap which does exist in these thin films is masked by the vibrational modes of the overlayer (peaks below 200 meV). Moreover, the vibrational peaks in Figs. 5(b)–5(d) are on a smooth background of electronic excitations which has an intensity between one and two orders of magnitude higher than that of the background in the clean metallic substrates or in bulk C_{60} [Fig. 5(a)]. The strong continuum of electronic excitations, reminiscent of that of the graphite (0001) surface,[49] indicates that the gap in the electronic excitation spectrum in the C_{60} monolayers, if it exists, is less than 100 meV and/or masked by the tail of the elastic peak. The spectra in Figs. 7(b) and 7(c) of C_{60} monolayers on the noble-metal surfaces also show a strong feature at about 0.8 eV which can only be attributed to low-energy electronic excitations of the C_{60} layer.

If we assume that the C_{60} layer does not interact with the substrate, the loss spectrum can be calculated using a two-layer model[25] and the dielectric functions of the substrate[50] and bulk C_{60}.[46] The result of these calculations for a monolayer film of C_{60} on Au(110), using the experimental geometry and an analyzer acceptance angle of 2°, is shown in Fig. 8. The spectrum shows very low intensity below 2 eV and sharp structures which can be attributed to C_{60} plus a contribution from the Au surface plasmon above 2 eV. The spectrum is similar to that from a C_{60} multilayer on Au(110) [Fig. 6(a)], apart from the absence of the feature at ≈ 2 eV, which corresponds to a dipole-forbidden transition. The peak at 0.8 eV appears in the computed loss spectra only if new interband

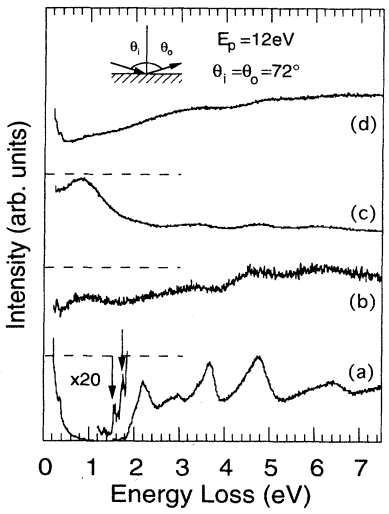

FIG. 7. Low-energy electronic excitations of (a) a multilayer of C_{60} (arrows indicate excitonic losses), and monolayers of C_{60} on (b) Au(110), (c) polycrystalline Ag, and (d) Ni(110). The absence of the band gap and excitons in the monolayers adsorbed at metal surfaces and the broadening of higher-lying electronic transitions indicate a metallic C_{60} film. The zero levels of the spectra are shown by dotted lines.

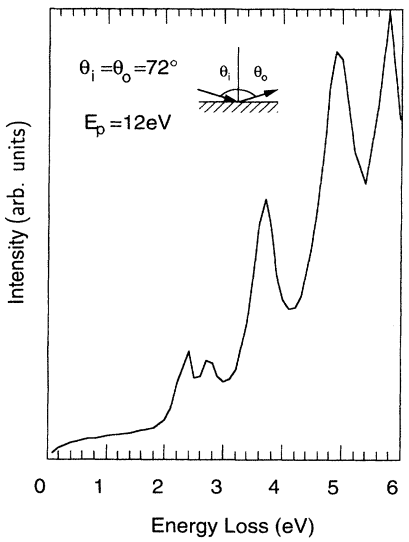

FIG. 8. Calculated surface loss function of a neutral C_{60} monolayer on a Au(110) substrate, for the same geometry (72° incidence and acceptance) and primary beam energy (12 eV) used to obtain the experimental spectra. A spectrometer acceptance angle of 2° was used. The C_{60} losses dominate the spectrum but are similar to those of a multilayer rather than a monolayer film, which indicates that the dielectric function of a C_{60} monolayer is strongly perturbed by the substrate. Note the absence of the dipole-forbidden loss feature at about 2.2 eV.

transitions and a low-energy Drude-like contribution to the overlayer dielectric function, similar to that observed in Rb_1C_{60}, K_3C_{60}, and K_4C_{60},[36] is included. The weak shoulder at 1 eV in the loss spectrum of C_{60} on Ni(110) could also arise from the large peak in the surface loss function of the substrate at this energy.[50] The calculations based on the two-layer model support the finding that the loss spectra are primarily derived from the electronic excitations in the C_{60} layer in the scattering geometry and at the primary beam energies used to acquire the data. Finally, a comparison of the higher-energy loss peaks for the multilayer C_{60} and the monolayers on all the substrates shows a broadening of the C_{60} loss peaks, a strong indication of metallicity. The metallic nature of the electronic excitations provides qualitative support for our estimation of molecular charge states, which would lead to a partial filling of the C_{60} lowest unoccupied molecular orbital (LUMO) derived band, and in the absence of band splitting due to electron correlation effects[51,52] to a metallic film.

SUMMARY

In conclusion, we have used vibrational spectroscopy to provide a quantitative estimate of the charge state of C_{60} molecules adsorbed on three metal surfaces. We find that the charge state of C_{60} molecules adsorbed onto a metal surface is strongly dependent upon the type of metal, but rather independent of the work function, with 1 ± 1 and 2 ± 1 electrons transferred to each C_{60} molecule for adsorption on the noble and transition metals, respectively. The lack of dependence of charge transfer on the work function of the metal surface [the work function of Ni(110) is between that of Au(110) and polycrystalline Ag] is consistent with the proposal that the transfer of charge arises through the formation of a chemical bond between the adsorbed C_{60} and the metal surface.[39] The assignments of charge state are given qualitative support by the electronic excitations of the fullerene overlayers: in contrast to a multilayer film or the bulk, the electronic structure of a C_{60} monolayer adsorbed at the surfaces investigated in this paper is clearly metallic.

We have also carried out LEED studies to determine the structure adopted by a C_{60} monolayer, and a detailed investigation of the early stages of C_{60} growth on the Ni(110) surface has been made. In the low-coverage regime, in particular, we find that the overlayer structure on Ni(110) differs strongly from that seen on other metal surfaces. This difference is determined by the relative strengths of the substrate-adsorbate and adsorbate-adsorbate interactions, information about which can be gleaned from the fullerene charge state. It is the stronger interaction between the adsorbed C_{60} and the Ni(110) surface than for the noble-metal surfaces, evidenced by the greater degree of charge transfer in the former, that leads to the formation of the rectangular Ni(110)-(5×3) C_{60} phase. The molecular charge state is found to be the same, to within experimental error, for all the phases observed on Ni(110), indicating that the charge transfer from the surface is not sensitively dependent on the structure adopted by the overlayer, and thus the coordination of the adsorbed molecules to the surface.

ACKNOWLEDGMENTS

The authors would like to thank Stefano Cerasari for assistance in acquiring the data for C_{60} on Au(110), and Cinzia Cepek for the program used to calculate the loss functions for the two-layer model. M.R.C.H. and R.E.P. would also like to thank the U.K. EPSRC and the Royal Society for financial support.

[1]P. A. Lane, L. S. Swanson, Q.-X. Ni, J. Shinar, J. P. Engel, T. J. Barton, and L. Jones, Phys. Rev. Lett. **68**, 887 (1992).
[2]G. F. Bertsch, A. Bulgac, D. Tománek, and Y. Wang, Phys. Rev. Lett. **67**, 2690 (1991).
[3]W. Y. Ching, M.-Z. Huang, Y.-N. Xu, W. G. Harter, and F. T. Chan, Phys. Rev. Lett. **67**, 2045 (1991).
[4]P. J. Benning, J. L. Martins, J. H. Weaver, L. P. F. Chibante, and R. E. Smalley, Science **252**, 1417 (1991).
[5]G. K. Wertheim, J. E. Rowe, D. N. E. Buchanan, E. E. Chaban, A. F. Hebard, A. R. Kortan, A. V. Makhija, and R. C. Haddon, Science **252**, 1419 (1991).
[6]C. T. Chen, L. H. Tjeng, P. Rudolf, G. Meigs, J. E. Rowe, J. Chen, J. P. Macauley, Jr., A. B. Smith III, A. R. McGhie, W. J. Romanow, and E. W. Plummer, Nature **352**, 603 (1991).
[7]A. F. Hebard, M. J. Rosseinsky, R. C. Haddon, D. W. Murphy, S. H. Glarum, T. T. M. Palstra, A. P. Ramirez, and A. R. Kortan, Nature **350**, 600 (1991).
[8]M. J. Rosseinsky, A. P. Ramirez, S. H. Glarum, D. W. Murphy, R. C. Haddon, A. F. Hebard, T. T. M. Plastra, A. R. Kortan, S. M. Zahurak, and A. V. Makhija, Phys. Rev. Lett. **66**, 2830 (1991).
[9]K. Tanigaki, T. W. Ebbeson, S. Saito, J. Mizuki, J. S. Tsai, Y. Kubo, and S. Kuroshima, Nature **352**, 222 (1991).
[10]K. Prassides, C. Christides, I. M. Thomas, J. Mizuki, K. Tanigaki, I. Hirosawa, and T. W. Ebbeson, Science **263**, 950 (1994).
[11]M. Kraus, S. Gärtner, M. Baenitz, M. Kanowski, H. M. Vieth, C. T. Simmons, W. Krätschmer, V. Thommen, H. P. Lang, H.-J. Güntherodt, and K. Lüders, Europhys. Lett. **17**, 419 (1992).
[12]H. B. Michaelson, in *CRC Handbook of Chemistry and Physics,* 74th ed., edited by D. R. Lide and H. P. R. Fredrikse (Chemical Rubber, London, 1993).
[13]J. K. Gimzewski, S. Modesti, and R. R. Schlittler, Phys. Rev. Lett. **72**, 1036 (1994).
[14]J. K. Gimzewski, S. Modesti, T. David, and R. R. Schlittler, J. Vac. Sci. Technol. B **12**, 1942 (1994).
[15]K. Motai, T. Hashizume, H. Shinohara, Y. Saito, H. W. Pickering, Y. Nishina, and T. Sakurai, Jpn. J. Appl. Phys. **32**, L150 (1993).
[16]E. I. Altman and R. J. Colton, Surf. Sci. **279**, 49 (1992).
[17]E. I. Altman and R. J. Colton, Surf. Sci. **295**, 13 (1993).
[18]J. Bohr, D. Gibbs, S. K. Sinha, W. Krätschmer, G. van Tendeloo, E. Larsen, H. Egsgaard, and L. E. Berman, Europhys.

Lett. **17**, 327 (1992).
[19]Y. Kuk, D. K. Kim, Y. D. Suh, K. H. Park, H. P. Noh, S. J. Oh, and S. K. Kim, Phys. Rev. Lett. **70**, 1948 (1993).
[20]M. R. C. Hunt and R. E. Palmer, Surf. Rev. Lett. (to be published).
[21]Y. Z. Li, J. C. Patrin, M. Chander, J. H. Weaver, L. P. F. Chibante, and R. E. Smalley, Science **252**, 547 (1991).
[22]S. Modesti *et al.* (unpublished).
[23]S. Fölsch, T. Maruno, A. Yamashita, and T. Hayashi, Surf. Sci. **294**, L959 (1993).
[24]D. E. Weeks and G. Harter, Chem. Phys. Lett. **144**, 366 (1988).
[25]H. Ibach and D. L. Mills, *Electron Energy Loss Spectroscopy and Surface Vibrations* (Academic, New York, 1982).
[26]G. Gensterblum, L.-M. Yu, J.-J. Pireaux, P. A. Thiry, R. Caudano, J.-M. Themlin, S. Bouzidi, F. Coletti, and J.-M. Debever, Appl. Phys. A **56**, 175 (1993).
[27]D. S. Bethune, G. Meijer, W. C. Tang, H. J. Rosen, W. G. Golden, H. Seki, C. A. Brown, and M. S. de Vries, Chem. Phys. Lett. **179**, 181 (1991).
[28]T. Pichler, M. Matus, and H. Kuzmany, Solid State Commun. **86**, 221 (1993).
[29]S. J. Duclos, R. C. Haddon, S. Glarum, A. F. Hebard, and K. B. Lyons, Science **254**, 1625 (1991).
[30]K.-A. Wang, Y. Wang, P. Zhou, J. M. Holden, S.-L. Ren, G. T. Hager, H. F. Ni, P. C. Eklund, G. Dresselhaus, and M. S. Dresselhaus, Phys. Rev. B **45**, 1955 (1992).
[31]S. J. Chase, W. S. Bacsa, M. G. Mitch, L. J. Pilione, and J. S. Lannin, Phys. Rev. B **46**, 7873 (1992).
[32]X. Q. Wang, C. Z. Wang, and K. M. Ho, Phys. Rev. B **48**, 1884 (1993).
[33]J. Yu, L. Bi, R. K. Kalia, and P. Vashishta, Phys. Rev. B **49**, 5008 (1994).
[34]M. J. Rice and H.-Y. Choi, Phys. Rev. B **45**, 10 173 (1992).
[35]J. Kohanoff, W. Andreoni, and M. Parrinello, Chem. Phys. Lett. **198**, 472 (1992).
[36]T. Pichler, R. Winkler, and H. Kuzmany, Phys. Rev. B **49**, 15 879 (1994).
[37]S. Modesti, S. Cerasari, and P. Rudolf, Phys. Rev. Lett. **71**, 2469 (1993).
[38]W. Andreoni, F. Gygi, and M. Parrinello, Phys. Rev. Lett. **68**, 823 (1992).
[39]A. J. Maxwell, P. A. Brühwiler, A. Nilsson, N. Mårtensson, and P. Rudolf, Phys. Rev. B **49**, 10 717 (1994).
[40]Y. Zhang, G. Edens, and M. J. Weaver, J. Am. Chem. Soc. **113**, 9395 (1991).
[41]R. L. Garrell, T. M. Herne, C. A. Szafranski, F. Diederich, F. Ettl, and R. L. Whetten, J. Am. Chem. Soc. **113**, 6302 (1991).
[42]T. R. Ohno, Y. Chen, S. E. Harvey, G. H. Kroll, J. H. Weaver, R. E. Haufler, and R. E. Smalley, Phys. Rev. B **44**, 13 747 (1991).
[43]A. Sellidj and B. E. Koel, J. Phys. Chem. **97**, 10 076 (1993).
[44]M. R. C. Hunt *et al.* (unpublished).
[45]J. W. Keller and M. A. Coplan, Chem. Phys. Lett. **193**, 89 (1992).
[46]E. Sohmen, J. Fink, and W. Krätschmer, Europhys. Lett. **17**, 51 (1992).
[47]Y. Wang, J. M. Holden, A. M. Rao, W.-T. Lee, X. X. Bi, S. L. Ren, G. W. Lehman, G. T. Hager, and P. C. Eklund, Phys. Rev. B **45**, 14 396 (1992).
[48]L.-Q. Jiang and B. E. Koel, Phys. Rev. Lett. **72**, 140 (1994).
[49]R. E. Palmer, J. F. Annett, and R. F. Willis, Phys. Rev. Lett. **58**, 2490 (1987).
[50]J. H. Weaver and H. P. R. Fredrikse, in *CRC Handbook of Chemistry and Physics* (Ref. 12).
[51]R. W. Lof, M. A. van Veenendaal, B. Koopmans, H. T. Jonkman, and G. A. Sawatzky, Phys. Rev. Lett. **68**, 3924 (1992).
[52]P. A. Brühwiler, A. J. Maxwell, P. Rudolf, C. D. Gutleben, B. Wästberg, and N. Mårtensson, Phys. Rev. Lett. **71**, 3721 (1993).

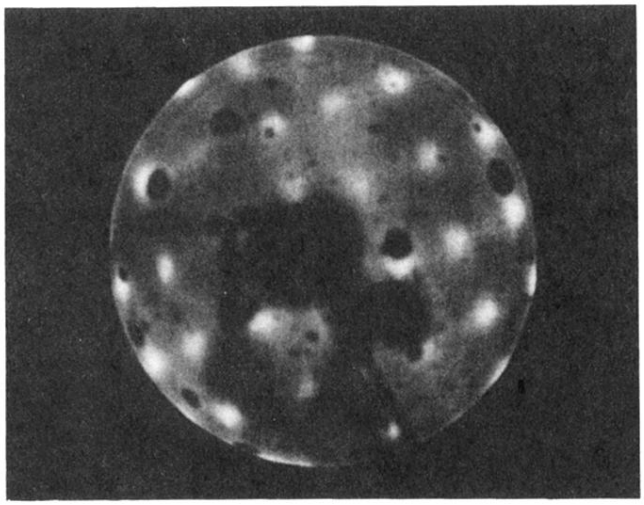

(a)

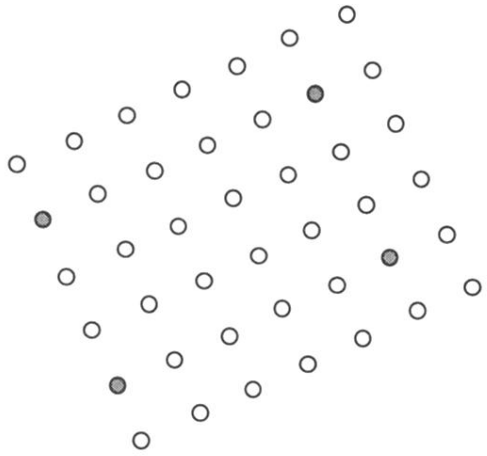

(b)

FIG. 1. (a) LEED pattern and (b) schematic of (5×3) C_{60}/Ni(110). Shaded circles represent the positions of diffraction spots from the clean Ni(110) surface. The incident beam energy was 26 eV.

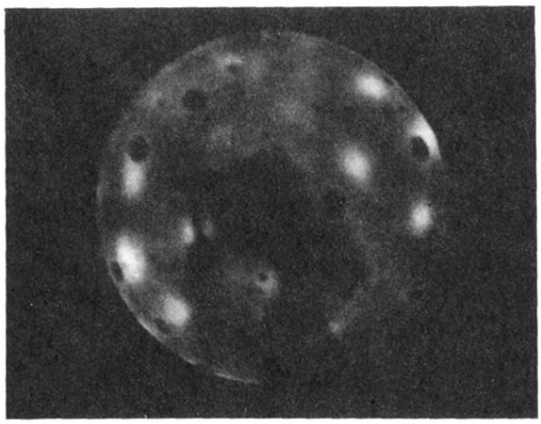

(a)

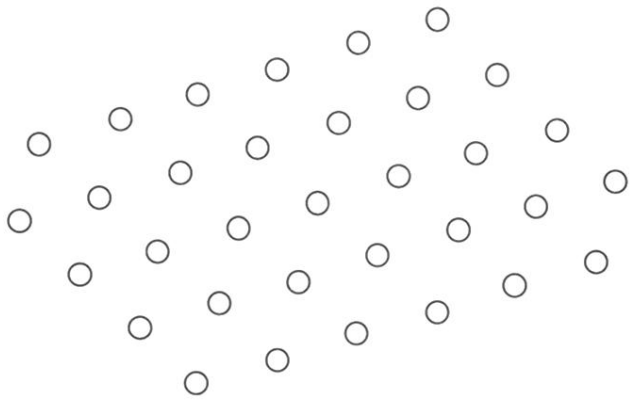

(b)

FIG. 3. (a) LEED pattern and (b) schematic of the QH1 phase of C_{60}/Ni(110). Incident beam energy was 24 eV.